Macromolecules

Article

pubs.acs.org/Macromolecules

Advantages of Block Copolymer Synthesis by RAFT-Controlled Dispersion Polymerization in Supercritical Carbon Dioxide

James Jennings,[†] Mariana Beija,[†] Jeremy T. Kennon,[†] Helen Willcock,[‡] Rachel K. O'Reilly,[‡] Stephen Rimmer,[§] and Steven M. Howdle*[,†]

[†]School of Chemistry, University Park, Nottingham NG7 2RD, U.K.

[‡]Department of Chemistry, University of Warwick, Gibbet Hill, Coventry CV4 7AL, U.K.

[§]Department of Chemistry, University of Sheffield, Sheffield S3 7HF, U.K.

Supporting Information

ABSTRACT: Reversible addition−fragmentation chain transfer (RAFT)-controlled block copolymer synthesis using dispersion polymerization in supercritical carbon dioxide ($scCO_2$) shows unprecedented control over blocking efficiency. For PMMA-*b*-PBzMA and PMMA-*b*-PSt the blocking efficiency was quantified by measuring homopolymer contaminants using the techniques of GPC deconvolution, gradient polymer elution chromatography (GPEC), and GPC dual RI/UV detection. A new, promising method was also developed which combined GPC deconvolution and GPEC. All techniques showed that blocking efficiency was significantly improved by reducing the radical concentration and target molecular weight. Estimated values agreed well with (and occasionally exceeded) theory for PMMA-*b*-PBzMA. The heterogeneous process in $scCO_2$ appeared to cause little or no further hindrance to the block copolymerization procedure when reaction conditions were optimized. High blocking efficiencies were achieved (up to 82%) even at high conversion of MMA (>95%) and high molecular weight. These data compare favorably to numerous published reports of heterogeneous syntheses of block copolymers.

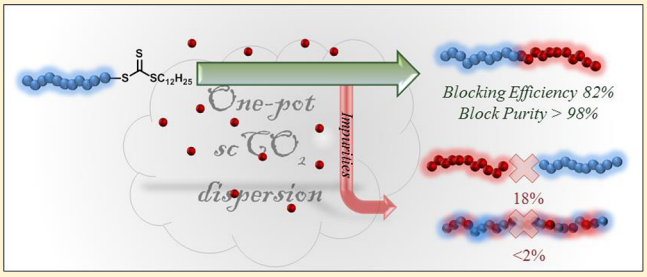

INTRODUCTION

Great interest in block copolymer synthesis has been stimulated by their fascinating phase separation behavior. The bond between the two blocks prevents macroscopic phase separation, and so the dimensions of the polymer chains result instead in formation of nanoscale domains. These domains can be in the form of a range of morphologies including lamellar, bicontinuous, cylindrical, and spherical. By exploiting this self-assembly, block copolymers have found application in areas as diverse as lithography,[1] photonics,[2,3] electronics,[4] membranes,[5] and nanoreactors,[6] alongside more traditional applications such as surfactants[7] and thermoplastic elastomers,[8] and thus are an important class of advanced material. Block copolymer synthesis has evolved recently, with traditional living anionic polymerization methods being rapidly replaced by controlled/pseudoliving radical polymerizations (CRP). The driving forces are the requirement for less stringent, more industrially applicable conditions as well as access to a wider range of monomers allowing synthesis of a more structurally diverse range of polymers.[9] Indeed, some industrial plants already adopt CRP for synthesis of specialty polymer products.[10]

Carrying out polymer synthesis in a two-phase system provides many process advantages, and heterogeneous polymerizations (including dispersion, emulsion, suspension, and precipitation) are used widely in industry.[11] Of particular importance are the improved heat dissipation, increased rates of reaction, ease of product recovery, and use of environmentally friendly solvents that are thus provided. Heterogeneous CRP techniques have been developed for systems in which the continuous phase is water,[12] alcohol,[13] and $scCO_2$.[14] Furthermore, the living nature of CRP has been exploited for block copolymer syntheses in aqueous emulsion polymerizations by RAFT,[8,15−19] nitroxide-mediated polymerization (NMP),[20,21] various forms of atom transfer radical polymerization (ATRP),[22,23] and other CRP methods.[24−26] Some of these processes have been used to form nanostructured polymer particles by exploiting *in situ* block copolymer self-assembly.[19,20,22] Internally structured particles hold great potential for applications as diverse as drug delivery[27] and photonic crystals.[28]

Supercritical carbon dioxide ($scCO_2$) has been explored as a medium in which to conduct heterogeneous CRP via RAFT,[29] ATRP,[30] NMP,[31] iodine transfer polymerization (ITP),[32] and reversible chain transfer catalyzed polymerization (RTCP),[32] but attempts at block copolymer synthesis are few.[30,33,34] The unique solvent properties of $scCO_2$ ensure that it is an ideal

Received: May 20, 2013
Revised: July 29, 2013
Published: August 27, 2013

medium in which to carry out dispersion polymerization since many combinations of soluble-monomer and insoluble-polymer exist. We recently reported the one-pot RAFT-controlled synthesis of block copolymers in a dispersion polymerization in $scCO_2$ in which we exploited these solvent properties to synthesize a diverse range of nanostructured block copolymer particles.[33]

Block copolymer synthesis in heterogeneous media maintains a low viscosity and good heat transfer even at high monomer conversion and thus allows simplification of the process by use of a one-pot method. However, a significant drawback of a one-pot method is that the purity of the block copolymer product can be compromised by loss of blocking efficiency and/or the formation of tapered blocks (Figure 1).

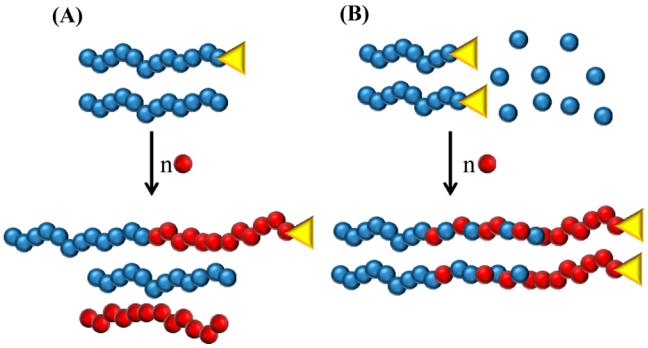

Figure 1. Schematic depicting impurities that can arise from one-pot block copolymer synthesis by controlled radical polymerization: (A) loss of chain-end functionality leading to dead chains and growth of new chains leads to low blocking efficiency and (B) the presence of unreacted monomer results in a tapered block at the center and loss of block interface definition.

In all CRP methods, the occurrence of radical−radical termination and chain transfer means that the process is never truly as living as a well-conducted anionic polymerization. Termination and chain transfer that occur during polymerization of the first block result in nonfunctional, "dead" chains that are not converted to block copolymer on addition of the second monomer (Figure 1A). In addition, homopolymer chains of second polymer can be initiated in some cases, especially if the order of block synthesis is not carefully selected in CRP.[35]

The quantity of block copolymer relative to homopolymer impurities is often referred to as "blocking efficiency", but a full evaluation of this is seldom addressed. Such data could be particularly important where the presence of homopolymer influences the block copolymer self-assembly. For example, Kagawa et al. found that a high loading of homopolymer caused loss of desirable phase separated morphology in block copolymer particles.[22] Furthermore, homopolymer contamination has been found to affect the mechanical properties of thermoplastic elastomers synthesized by CRP.[36] Such homopolymer can be removed from the final block copolymer, but this adds processing steps and is not facile if the two blocks have similar solubilities.

Additionally, if unreacted monomer remains after the first block synthesis, copolymerization with the second monomer will result in a central "tapered" segment (Figure 1B). This loss of the sharp block−block definition is undesirable as it results in a lower polymer−polymer interaction parameter and potentially the loss of phase-separated morphology.[20] In order to minimize tapered block formation, the unreacted monomer must be removed after the first step by a tedious method such as dialysis.[18] Alternatively, the reaction can be taken to high conversion, but this leads to increased termination reactions, lower livingness, and a decrease in blocking efficiency. Hence, the formation of block copolymers with high blocking efficiency and low tapered content is not facile in a one-pot synthesis.

A number of techniques exist for quantifying the blocking efficiency, three of which are adopted in this study. (1) *GPC deconvolution:* GPC traces are split into block copolymer and homopolymer components using a Gaussian fitting algorithm and peak areas are integrated.[37,38] (2) *Gradient solvent separation:* Block copolymers and homopolymers are physically separated by exploiting the different solubilities of the two components. Techniques such as gradient polymer elution chromatography (GPEC)[39,40] or liquid adsorption chromatography (LAC)[20] have been utilized for this. (3) *GPC dual detection:* Comparison of GPC traces from two detectors in which one block is invisible to one of the detectors. For example, Kitayama et al. used UV detection (254 nm) at which the block copolymer PMMA-*b*-PBzMA was visible but PMMA homopolymer was invisible. The area of the UV peak relative to the RI peak was then used to calculate blocking efficiency.[25]

The blocking efficiency of the block copolymer syntheses in $scCO_2$ was previously evaluated by GPC deconvolution analysis.[33] Here we extend this study to measure blocking efficiency at varying initiator concentrations and molecular weight to assist optimization. We utilized three reported methods for quantification and devised a new method combining GPC deconvolution and GPEC, while tapered block content was quantified by ^{1}H NMR analysis. The results obtained are compared to theory and with similar heterogeneous polymerizations in the literature.

EXPERIMENTAL SECTION

Materials. *S*-Dodecyl-*S*′-(α,α′-dimethyl-α″-acetic acid) trithiocarbonate (DDMAT) was synthesized following a literature procedure.[41] α-Azobis(isobutyronitrile) (AIBN, Wako, 97%) was purified by recrystallizing twice in methanol. Methyl methacrylate (MMA, Fisher, >99%), benzyl methacrylate (BzMA, Alfa Aesar, 98%), and styrene (St, Alfa Aesar, 99%) were purified by eluting through a basic alumina column. Poly(dimethylsiloxane)−monomethyl methacrylate (PDMS−MA, ABCR, M_n = 10 kg mol^{-1}), $CDCl_3$ (Aldrich), HPLC grade THF, hexane, and triethylamine (Fisher) were used without further purification.

One-Pot Block Copolymer Synthesis. In a typical procedure targeting a symmetrical block copolymer with 100 kg mol^{-1}, a high-pressure autoclave (60 mL) was charged with RAFT agent (DDMAT, 0.150 mmol), AIBN (0.075 mmol), and macromonomer stabilizer (PDMS-MA, 5 wt % of total monomer mass). The autoclave was degassed by purging with CO_2 at 2 bar for 60 min, while MMA (74.8 mmol) was degassed by bubbling with argon, before being added to the autoclave. The vessel was then sealed and pressurized to 50 bar, heated to 65 °C, and the pressure topped up to 275 bar. The reaction mixture was stirred for 24 h, and a sample was taken from the autoclave by needle valve. The sample was characterized by GPC (M_n = 51 kg mol^{-1} where target was 50 kg mol^{-1}, $Đ$ = 1.22). BzMA (42.5 mmol) was degassed for 30 min and transferred to a vial containing AIBN (0.037 mmol) to be degassed for a further 10 min. The pressure in the autoclave was then reduced to <200 bar, and the monomer and initiator were added through the top of the vessel using an HPLC pump (Gilson 305). After a further 48 h of polymerization, the temperature was lowered to ambient and the pressure reduced by venting the autoclave over a period of ∼30 min. All products were collected as dry, pale yellow, and free-flowing powders.

dx.doi.org/10.1021/ma401051e | *Macromolecules* 2013, 46, 6843−6851

Table 1. Characteristics of PMMA-*b*-PBzMA Synthesized Using Different Amounts of AIBN[a]

MMA (mmol)	AIBN (equiv) step 1	AIBN (equiv) step 2	$M_{n,theo}$[b] (kg mol^{-1})	$M_{n,exp}$[c] (kg mol^{-1})	$Đ$[c]	blocking efficiency		
						deconv	GPEC	dual detection
75	2.5	0.2	41	52	1.29	33	63	81
75	1	0	63	63	1.41	54	64	81
75	0.5	0.25	69	77	1.38	63	85	87
94	0.25	0.2	78	83	1.35	67	86	88
112	0.125	0.125	86	92	1.24	76	90	91

[a]All reactions carried out with equal weight ratio MMA:BzMA, 5 wt % PDMS−MA (with respect to both monomers) in 60 mL autoclave for 24 h (MMA polymerization) and 48 h (BzMA polymerization) at 65 °C and 275 bar. [b]Calculated from eq 5. [c]Determined by GPC in THF against PMMA standards.

Table 2. Characteristics of PMMA-*b*-PSt Synthesized Using Different Amounts of AIBN[a]

MMA (mmol)	AIBN (equiv) step 1	AIBN (equiv) step 2	$M_{n,theo}$[b] (kg mol^{-1})	$M_{n,exp}$[c] (kg mol^{-1})	$Đ$[c]	blocking efficiency		
						deconv	GPEC	dual detection
75	2.5	0.2	25	35	1.76	30	72	79
75	1	0.36	32	47	1.85	37	82	78
75	0.5	0.67	35	54	1.69	45	86	78
94	0.25	0.5	40	50	1.51	51	88	80
112	0.125	0.4	44	55	1.40	57	93	83

[a]All reactions carried out with equal weight MMA:St, 5 wt % PDMS-MA (with respect to both monomers) in 60 mL autoclave for 24 h (MMA polymerization) and 72 h (St polymerization) at 65 °C and 275 bar. [b]Calculated from eq 5. [c]Determined by GPC in THF against PMMA standards.

Analysis. ^{1}H NMR was carried out in $CDCl_3$ on a Bruker DPX 300 MHz spectrometer. Molecular weight and dispersity were determined on a Polymer Laboratories PL GPC 120 with two columns (300 mm, PolarGel-M), a guard column, and a differential refractive index (RI) detector calibrated with PMMA narrow standards (PL). Samples were run in THF at ∼5 mg/mL at a flow rate of 1 mL/min. GPC dual detection was carried out on a PL GPC 50 with two columns (PLgel Mixed-D) and a guard column calibrated with PMMA narrow standards (PL). Samples were run at ∼2 mg/mL in THF with 2 vol % triethylamine at a flow rate of 1 mL/min. Detection was achieved with both an in-built RI and a Shimadzu SPD-M20A prominence diode array (PDA) detector for UV analysis at 268 and 309 nm. GPEC separation was carried out by dissolving samples in a THF/hexane mixture (∼0.1 mg/mL) and injecting into a 0.5 mL/min flow of pure hexane. An Agilent 1100 series pump was used to change the solvent composition to THF over a period of 10 min, followed by isocratic conditions for 5 min. Separation was achieved via a Nova Pak silica column (3.9 × 150 mm). Detection was carried out with an evaporative light scattering detector (ELS, Polymer Laboratories PL-ELS 1000).

Quantification of Blocking Efficiency. *GPC Deconvolution.* GPC traces were plotted as log MW vs (RI response/MW) and then split into three peaks: the block copolymer, the homopolymer PMMA (hPMMA), and unreacted PDMS stabilizer (Supporting Information Figure 1). The different dn/dc values for each component had to be taken into account when integrating. The dn/dc values were taken from the literature (0.086 for PMMA[42] and 0.186 for PSt[42] in THF at 25 °C, 0.141 for PBzMA[43] in THF at 40 °C) and calculated based on the weight fraction of the two blocks (w_{P1}, w_{P2}) calculated by ^{1}H NMR (eq 1).[37]

$$\left(\frac{dn}{dc}\right)_{BCP} = w_{P1}\left(\frac{dn}{dc}\right)_{P1} + w_{P2}\left(\frac{dn}{dc}\right)_{P2} \quad (1)$$

To estimate the blocking efficiency ($B_{Eff,deconv}$), the areas of the two peaks (A_{block} and A_{PMMA}) were obtained via Origin Peak Analyzer and were normalized with respect to their dn/dc (eq 2).

$$B_{Eff,deconv} = \frac{A_{BCP}/\left(\frac{dn}{dc}\right)_{BCP}}{A_{BCP}/\left(\frac{dn}{dc}\right)_{BCP} + A_{PMMA}/\left(\frac{dn}{dc}\right)_{PMMA}} \quad (2)$$

Reproducibility was ensured with five deconvolutions to obtain an average and standard deviation (1−2% in all cases). This method follows closely that of Bartels et al.[37] but uses the modified GPC trace (in which RI response is divided by MW) to allow easier peak fitting. The method was validated by analysis of known quantities of polymer standards.

GPEC. Blocking efficiency was calculated simply from the area of block copolymer peak relative to total area of polymer peaks (eq 3). For example, for PMMA-*b*-PBzMA

$$B_{Eff,GPEC} = \frac{A_{PMMA\text{-}b\text{-}PBzMA}}{A_{PMMA\text{-}b\text{-}PBzMA} + A_{PMMA} + A_{PBzMA}} \quad (3)$$

Blocking efficiency values calculated by this method were not absolute because of the complex nature of the ELS response for polymers and its sensitivity to structure.[44]

GPC Dual Detection. Since PBzMA, PSt, and the RAFT agent all have strong UV absorptions, they could be selectively detected using a UV detector. UV (268 and 309 nm) and RI traces were first scaled to equivalent number distributions by dividing response by (MW)^2 (RI and 268 nm) or MW (UV 309 nm) and then overlapped at the high molecular weight end, following the method published by Okubo.[23,24] After overlap of two UV and RI traces, it was apparent that the UV 268 nm trace had a larger area than the UV 309 nm trace and even the RI trace in some cases (Figure 4). This was attributed to significant presence of UV−vis second block homopolymers. Thus, calculations were carried out on UV 309 nm traces only (example in Supporting Information Figure 3). After overlapping, the relative area of the UV peak (A_{UV}) to the area of the RI peak (A_{RI}) determined the blocking efficiency (eq 4).

$$B_{Eff,dual} = \frac{A_{UV}}{A_{RI}} \quad (4)$$

RESULTS AND DISCUSSION

As we reported previously, some quantity of hPMMA remained from the block copolymer synthesis in $scCO_2$,[33] which is fully anticipated for the pseudoliving RAFT process. In addition, the use of a heterogeneous dispersion system could potentially lead to process complications such as diffusion of control agent out into the continuous phase,[45] which could further decrease the

dx.doi.org/10.1021/ma401051e | Macromolecules 2013, 46, 6843−6851

livingness and thus purity of the block copolymer. Quantifying and maximizing blocking efficiency was the priority in this study, and initial optimization was effected by decreasing the initiator concentration.

Blocking Efficiency: Effect of RAFT:Initiator. The concentration of initiator in the synthesis of a number of symmetrical block copolymers was tuned by changing the equivalents of AIBN relative to RAFT agent while maintaining constant monomer:RAFT ratio (500 for PMMA-*b*-PBzMA and 300 for PMMA-*b*-PSt in Tables 1 and 2, respectively). $M_{n,theo}$ was calculated taking into account the influence of initiator on molecular weight (eq 5) and assuming that conversion of both monomers was 100%, which was reasonable considering in all reactions conversion >98%. It was found that in all cases $M_{n,exp}$ was higher than $M_{n,theo}$. This was previously observed in the RAFT-controlled polymerization of MMA in $scCO_2$ and was explained by a lower than expected [I] caused by increased initiator−initiator terminations facilitated by the high diffusivity of $scCO_2$.[29] Alternatively, it has been observed that radical−radical terminations are slowed at high pressure,[46] which could also lead to an enhancement of livingness.

$$M_{n,theo} = \frac{[M]_1}{[R] + df[I](1 - e^{-k_d t})} m_{M1} + \frac{[M]_2}{[R] + df[I](1 - e^{-k_d t})} m_{M2} + m_{RAFT} \quad (5)$$

In which $[M]_1$, $[M]_2$ $[R]$, and $[I]$ are concentrations of monomers 1 and 2 and RAFT agent and initiator, respectively, d refers to the preferred mode of termination, f is initiator efficiency, and k_d is initiator decomposition rate constant calculated based on decomposition in $scCO_2$ in the presence of a cosolvent at 65 °C (see Supporting Information).[47]

As propagation rate of a polymerization is proportional to $[I]^{1/2}$, decreasing AIBN concentration would result in slowed polymerization kinetics. To compensate for this, more MMA and longer reaction times (24 h) were used when 0.125 and 0.25 equiv of AIBN were used to ensure complete conversion of MMA and to minimize the formation of tapered block. Initiator remaining after the first step was estimated based on decomposition of AIBN in $scCO_2$−solvent mixture at 65 °C (see Supporting Information) and an appropriate amount of further initiator added with the second monomer to allow complete polymerization in the reaction times. A higher concentration of initiator was added when using St in order to overcome the slower propagation.[42]

All three methods showed an increase in blocking efficiency as initiator concentration was decreased, indicating a decrease in termination reactions at lower radical concentration and hence a higher proportion of living PMMA. Furthermore, dispersity decreased as initiator concentration was decreased, concurrent with a visible reduction of the low molecular weight shoulder in the GPC (Figure 2). Dispersities of PMMA-*b*-PSt were higher than PMMA-*b*-PBzMA, which is consistent with the broader GPC traces resulting from the formation of large chains from PMMA-*b*-PSt, which undergoes termination by combination. Dispersities obtained here are comparable to other examples of heterogeneous syntheses (e.g., in a recent synthetic study by Okubo PMMA-*b*-PBzMA, $Đ$ = 1.32)[25] but typically higher than solution-based synthesis.

GPEC traces (Figure 3) showed peaks for both hPMMA and hPBzMA/hPSt (confirmed by comparison to homopolymer references (Supporting Information Figure 2)) with the block

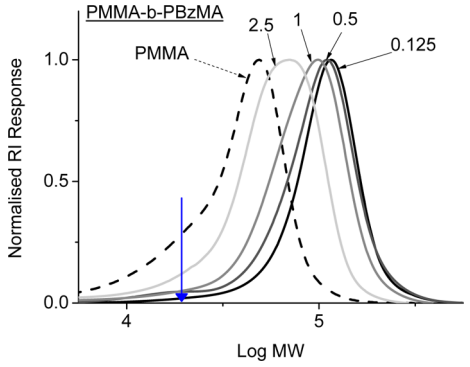

Figure 2. Stacked GPC traces of PMMA-*b*-PBzMA synthesized with a range of AIBN equivalents (amounts used for MMA polymerization noted on each trace). The low molecular weight shoulder diminished and GPC trace became more monomodal as AIBN concentration was decreased, indicating improvement of blocking efficiency. The blue arrow highlights the presence of PDMS−MA stabilizer at log MW ~ 4.3.

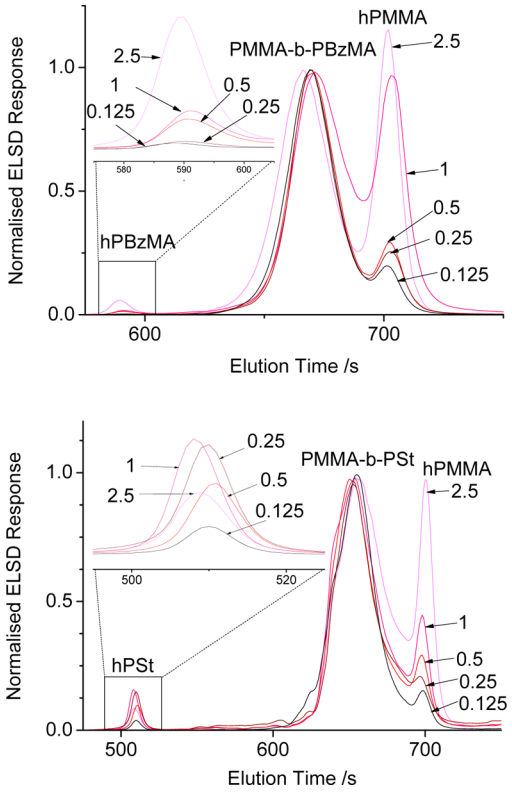

Figure 3. GPEC traces labeled with respective AIBN equivalents used in first block synthesis for PMMA-*b*-PBzMA copolymers (top) and PMMA-*b*-PSt copolymers (bottom). Figure insets are centered on hPBzMA/hPSt peaks, showing that homopolymers of both blocks were clearly present in all cases.

copolymer peak at intermediate retention time, as expected. The height of the hPMMA peak decreased with AIBN equivalents added, indicating an increase in blocking efficiency. The second block homopolymer was present even at the lower concentration of initiator, which suggests that it is unavoidable to some extent in such a RAFT polymerization.

In GPC dual detection, UV traces from PMMA-*b*-PSt revealed low molecular weight shoulders which suggested that block copolymer was not the only species being detected

dx.doi.org/10.1021/ma401051e | *Macromolecules* 2013, 46, 6843−6851

(Figure 4). As the peak appeared at a similar retention time as hPMMA, it was assumed that it was due to hPSt. The peak was

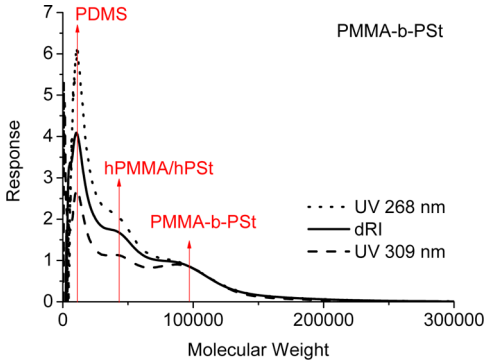

Figure 4. GPC dRI, UV 268 nm (benzyl), and 309 nm (RAFT) traces of PMMA-*b*-PSt overlapped at high molecular weight for blocking efficiency estimation. The data from UV GPC at 268 and 309 nm showed a significant quantity of hPSt in the same region as hPMMA in the dRI trace.

visible at both 268 and 309 nm, suggesting that the hPSt had RAFT functionality. This could occur if new chains were initiated early in the second stage of polymerization and added to/fragmented from the RAFT agent independently of the block copolymer chains. Any hPSt present in the final product would count toward the block copolymer peak and lead to overestimation of blocking efficiency by GPC dual detection, as has previously been postulated.[23]

Blocking Efficiency: Comparing Estimation Methods. Blocking efficiency estimates from all methods were plotted as a function of R:I (Figure 5). Clearly, values estimated by GPC deconvolution and GPEC showed a similar trend, but with significantly different absolute values. It is likely that the values from GPEC are reliable within one set of block copolymers, but the absolute values are not accurate because of the complex nature of the ELS response for block copolymers. Blocking efficiency calculated by GPC dual detection showed only a slight linear increase with R:I (Figure 5). In combination with the appearance of second block homopolymer in UV GPC traces, this suggested that these results were unreliable, and this method should be used with caution when determining blocking efficiency from a process. This also explained the lower blocking efficiency estimated for PMMA-*b*-PSt compared to PMMA-*b*-PBzMA from deconvolution, as the content of hPSt was higher than hPBzMA (also evident by GPEC and GPC dual detection). This was fully expected, since more initiator was added when using St which would likely lead to increased initiation of homopolymer chains of second monomer.

Thus, of the three methods, GPC deconvolution appeared to be the most reliable, as it made the fewest assumptions.

Blocking Efficiency: Combined Estimation Method. In order to improve reliability of the blocking efficiency estimation, some assumptions of the different techniques could be overcome by combining methods. As mentioned before, the commonly used GPC dual detection method works on the assumption that all material in the UV trace is block copolymer.[23] In addition, GPC deconvolution assumes that the low molecular weight polymer peak derives only from hPMMA and that no homopolymer of the second block is present. Since the GPEC studies showed that second block homopolymer was certainly present, this assumption is clearly invalid.

It is likely that homopolymer of the second block (hPBzMA/hPSt) overlaps with the homopolymer shoulder in the GPC trace, which is supported by the GPC UV traces (Figure 4). As these copolymers have significantly different dn/dc values, this would lead to an error in estimation of blocking efficiency by GPC deconvolution. In order make the estimate more accurate, the homopolymer peak from GPC deconvolution was normalized with respect to both polymers. The fraction of PMMA and second block homopolymer which contributed to the low molecular weight peak ($f_{PMMA/P2}$) was measured from GPEC integration. Hence, eq 2 was modified to eq 6 to account for this.

$$B_{\mathrm{Eff,GPC/GPEC}} = \left\{A_{\mathrm{BCP}}/\left(\frac{\mathrm{d}n}{\mathrm{d}c}\right)_{\mathrm{BCP}}\right\} \Bigg/ \left\{A_{\mathrm{BCP}}/\left(\frac{\mathrm{d}n}{\mathrm{d}c}\right)_{\mathrm{BCP}} + \left(A_{\mathrm{PMMA}} f_{\mathrm{PMMA}}/\left(\frac{\mathrm{d}n}{\mathrm{d}c}\right)_{\mathrm{PMMA}}\right) + \left(A_{\mathrm{P2}} f_{\mathrm{P2}}/\left(\frac{\mathrm{d}n}{\mathrm{d}c}\right)_{\mathrm{P2}}\right)\right\} \quad (6)$$

Although values estimated by GPEC were not absolute, the relative areas of the two peaks would be fairly reliable as ELS detection is independent of chemical structure. In addition, it is

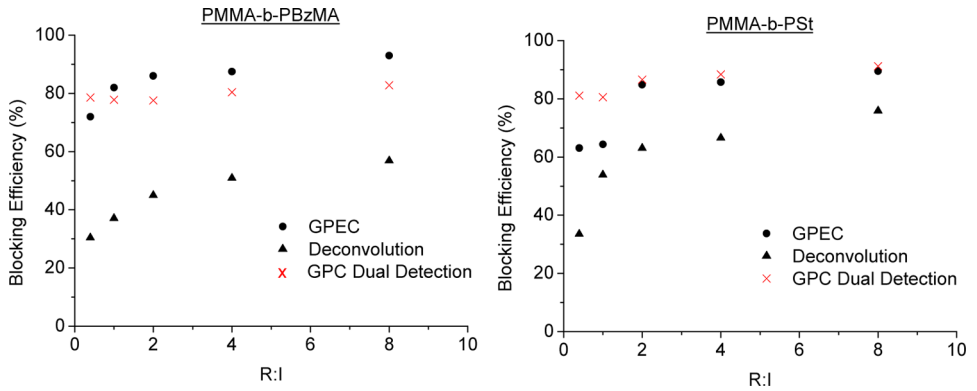

Figure 5. Comparison of blocking efficiency estimated from all methods as a function of R:I for PMMA-*b*-PBzMA and PMMA-*b*-PSt. Trends were similar for GPC deconvolution and GPEC but distinctly different for GPC dual detection, highlighting the limitation of this method for these systems.

dx.doi.org/10.1021/ma401051e | *Macromolecules* 2013, 46, 6843−6851

likely that response in the ELS detector has some dependence on molecular weight, which will no longer be a factor as both homopolymers were of similar molecular weight. Results from this calculation were compared to those from the original method (Table 3). For PMMA-*b*-PBzMA, there was little change in calculated blocking efficiency compared to the GPC deconvolution method, but a clear increase for PMMA-*b*-PSt. This was as anticipated, given the higher content of hPSt than hPBzMA. By combining GPEC and RI GPC deconvolution, fewer assumptions were made and the most accurate estimate was obtained.

Table 3. Blocking Efficiency Estimated by the GPC/GPEC Method Compared to the Standard Deconvolution Method

	PMMA-*b*-PBzMA		PMMA-*b*-PSt	
AIBN (equiv) step 1	$B_{Eff,deconv}$	$B_{Eff,GPC/GPEC}$	$B_{Eff,deconv}$	$B_{Eff,GPC/GPEC}$
2.5	33	34	30	32
1	54	54	37	39
0.5	63	63	45	48
0.25	67	67	51	55
0.125	76	76	57	59

Blocking Efficiency: Comparison to Theory. Next, we investigated how closely the RAFT process in $scCO_2$ followed what is theoretically predicted. To do this, it was assumed that the blocking efficiency from the process was closely related to the livingness of the first step of polymerization. Livingness can be estimated based on initial RAFT and initiator concentration ([I] and [RAFT]), initiator efficiency (f), decomposition rate constant (k_d), time (t), and preferred mode of termination (d) (eq 7).[48] The initiator efficiency and k_d were calculated from literature values for AIBN in $scCO_2$ in the presence of cosolvent at 65 °C[47] (see Supporting Information). A d value of 1.67 was used, as reported for methacrylate polymers which have a preference for termination by disproportionation.[48]

$$\text{livingness} = B_{Eff,theo} = \frac{[R]}{[R] + df[I](1 - e^{-k_d t})} \quad (7)$$

Blocking efficiencies estimated from the GPEC-deconvolution method (Table 3) were compared to results from eq 7 as a function of R:I (Figure 6).

The measured blocking efficiencies showed reasonable agreement with theory for PMMA-*b*-PBzMA, but much less so for PMMA-*b*-PSt, and deviation from theory increased at higher R:I. Crucially, the theoretical curve only takes into account first block homopolymer (hPMMA), which explains the significant deviation for PMMA-*b*-PSt in which a considerable quantity of hPSt was found. It is worth noting that the deconvolution method is not without fault, as the fitting procedure was carried out using symmetrical Gaussian curves, whereas in reality the peaks may have some tailing toward low molecular weight. If this was the case, blocking efficiency here was underestimated.

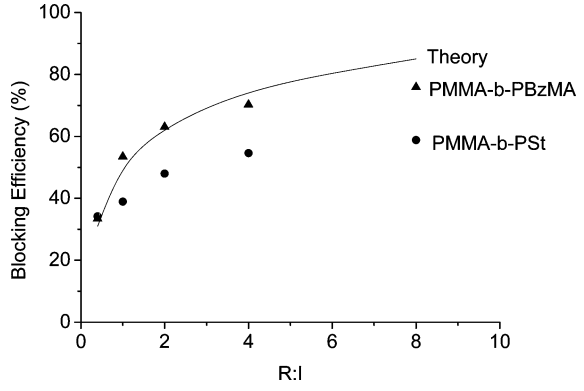

Figure 6. Blocking efficiencies estimated from GPC/GPEC method compared with theory as a function of R:I for block copolymers PMMA-*b*-PBzMA (▲) and PMMA-*b*-PSt (●).

Blocking Efficiency: Effect of Molecular Weight. Another possible contribution to the deviation of estimated from theoretical blocking efficiency could be the high molecular weights targeted in the process. Others have shown that an increase in first block DP has a detrimental effect on blocking efficiency for RAFT polymerization.[37,39] In addition, one theoretical study of ATRP estimated the dependence of livingness on molecular weight, conversion, and time. It was found that increasing each of these factors resulted in a decrease in livingness,[49] and furthermore, an MMA polymerization with a target DP of 500 taken to conversion greater than 95% in 24 h would have a theoretical livingness of ~70%. Hence, our PMMA-*b*-PBzMA polymerizations, which targeted the same high molecular weight polymers (Table 1, MMA target DP = 500) and achieved high conversion in a similar time scale, may have been at their limit of livingness at ~76%. In order to elucidate the molecular weight effect, blocking efficiencies of PMMA-*b*-PBzMA and PMMA-*b*-PSt with target DP of 300 and 500 were compared (Table 4).

Blocking efficiency was higher for block copolymers with lower target DP for PMMA-*b*-PBzMA and PMMA-*b*-PSt, confirmed in all cases by two different estimation techniques. One possible reason for this is that the decrease in DP significantly lowers the melt viscosity of PMMA (5.7 times lower).[50] Furthermore, the plasticization of the PMMA microparticles by $scCO_2$ could better facilitate access of the second monomer to the RAFT functional polymer.[51]

Tapered Block Quantification. In order to quantify any tapered block within the block copolymer structures, polymers with known quantities of tapered block were synthesized and characterized by ^{1}H NMR analysis. PMMA-*b*-PSt was synthesized in solution, but St was deliberately added before complete conversion of MMA (measured by ^{1}H NMR). Inspection of ^{1}H NMR of the resulting block copolymer revealed additional broad peaks in the region of 2.3−3.3 ppm (Supporting Information Figure 4). This region has also been reported for PMMA-*s*-PSt statistical copolymer,[52] suggesting that the polymer did indeed contain a central tapered block consisting of both monomers. The integration of this area relative to PMMA agreed well with PMMA conversion, which implied that these peaks arose from PMMA in a PSt environment. A similar experiment for PMMA-*b*-PBzMA revealed a peak at 3.45 ppm, which was assigned to a PMMA-*s*-PBzMA tapered block. For the $scCO_2$ synthesized block copolymers (Tables 1 and 2) detailed analysis revealed that, in all cases, tapered block content was very low (<2 wt %) relative to the entire block copolymer. This confirmed that MMA achieved high conversion, as GPC analysis suggested.

Comparison to Literature. The systems most comparable to our $scCO_2$ dispersion are heterogeneous block copolymer syntheses in which the first block forms a dispersed particle, to which the second monomer is added and polymerizes within the particle. A combination of both high blocking efficiency and

dx.doi.org/10.1021/ma401051e | Macromolecules 2013, 46, 6843−6851

Table 4. Effect of Target DP on Blocking Efficiency for PMMA-*b*-PBzMA and PMMA-*b*-PSt[a]

				blocking efficiency			
entry	block copolymer	AIBN (equiv) step 1	MMA target DP	theo[b]	deconv	GPEC	dual detection
1	PMMA−PBzMA	0.125	300	85	82		92
2			500		76		91
3	PMMA−PBzMA	0.5	300	63	66		90
4			500		63		87
5	PMMA−PSt	0.125	300	85	57	93	
6			500		52	88	

[a]All reactions carried out with equal weight ratio MMA:BzMA/St, 5 wt % PDMS−MA (with respect to both monomers) in 60 mL autoclave for 24 h (MMA polymerization) and 48 h (BzMA polymerization) or 72 h (St polymerization) at 65 °C and 275 bar. [b]Calculated from eq 7.

low block tapering is difficult to achieve in conventional emulsion, miniemulsion, and microemulsion syntheses.

In ATRP emulsion synthesis, Kitayama et al. reported blocking efficiencies up to 62%, calculated by the GPC dual detection method.[23,53] The low value was attributed to the high degree of bimolecular terminations occurring during the formation of the P^{i}BuMA seed.[23] In addition, their resulting block copolymers would most likely have tapered regions since second monomer was added after only ∼80% conversion of first monomer.

Block copolymer synthesis by NMP in an emulsion polymerization resulted in high blocking efficiency (>90%), measured by LAC analysis.[20] However, this was also likely to be at the expense of a tapered block at the center, since conversions of the first block were 55−89%, and no purification was carried out before adding the second monomer.

Monteiro and co-workers estimated blocking efficiencies of up to 90% for RAFT emulsion block copolymer synthesis, by a form of GPC dual detection.[16,18] However, homopolymer of the second block was not considered, which may have contributed to this high value. Dialysis was carried out in between polymerization steps to remove unreacted monomer and prevent the formation of a tapered block. Other studies have investigated RAFT heterogeneous synthesis of block copolymers, but many do not include a quantification of blocking efficiencies.[8,19]

Finally, Okubo and co-workers used organotellurium-mediated living radical polymerization (TERP)[24] and reversible chain transfer catalyzed polymerization (RTCP)[25] methods to synthesize block copolymers in emulsion. Blocking efficiency estimated by GPC dual detection was 75% and 88% for TERP and RTCP, respectively. Again, conversions achieved before addition of second monomer were low (80% and 64% for TERP and RTCP, respectively) which would likely result in a central tapered block.

It is clear that the blocking efficiencies obtained in $scCO_2$ (up to 82%) are comparable with, and often favorable to, those observed in other CRP reactions in heterogeneous media. Furthermore, the high conversion of the first block ensures that blocks are pure and have very low tapered regions (<2%) compared to most examples in the literature.

To explain the efficiency of the RAFT-$scCO_2$ syntheses, we propose that the $scCO_2$-induced plasticization of PMMA expands the particles, while high diffusivity allows access of second monomer to the polymerization *loci*. This effect is absent in heterogeneous polymerizations in water, in which mobility within the particles is only influenced by monomer swelling. Hence, seeding steps are required,[15] and many of these investigations use low-T_g polymers as the first block in the copolymer.[16,20,21,23,24] In addition, the degenerative chain transfer mechanism ensures the RAFT agent remains attached to a polymer chain throughout and thus will remain within the particle. Free species such as copper complexes (ATRP) or nitroxides (NMP) can diffuse out of the particle phase, which results in loss of control and/or livingness.[54]

One important process advantage of $scCO_2$ dispersion over aqueous emulsions is in the simplicity in separating polymer and continuous phase. Polymers can be immediately separated by release of pressure, which is more facile than time-consuming and high-temperature drying.

CONCLUSIONS

We have shown that the process of block copolymer synthesis in supercritical CO_2 dispersion is efficient and simple and results in production of high-purity block copolymers in a one-pot, solvent-free synthesis. Products were found to have dispersity that is relatively narrow for a heterogeneous synthesis and controlled molecular weight, indicative of a successful RAFT process. In addition, the blocking efficiency of the process was excellent when initiator concentration and target DP were lowered. Comparison with theory indicates that the process of carrying out block copolymer synthesis in $scCO_2$ dispersion creates little or no further hindrance to the blocking efficiency and may even exceed theory in some cases. Advantages over aqueous emulsion routes to block copolymers are apparent in both the procedure and the product purity, with blocking efficiency found to be higher than the majority of prior reports in the literature. In some circumstances, tuning the content of homopolymer in a block copolymer−homopolymer blend may be advantageous,[2] and here we present a simple method that could be exploited.

A novel method combining GPC deconvolution and GPEC provided the most accurate estimate of blocking efficiency, while the commonly used GPC dual detection was shown to have clear limitations when both homopolymers were present. This study also emphasizes the importance of effective quantification of blocking efficiency in block copolymer syntheses, as visual analysis is insufficient in providing evidence of pure block copolymers, and the effect of homopolymer contamination on the properties of the resulting material can be significant.

Along with the high-purity block copolymers formed, the $scCO_2$ dispersion route adheres to several principles of green chemistry: low waste, high atom economy, low toxicity of solvent, one-pot synthesis, and the avoidance of purification steps. We have already demonstrated exquisite control of the resulting nanostructured microparticle products,[33] thus opening up opportunity for a multitude of applications.

dx.doi.org/10.1021/ma401051e | *Macromolecules* 2013, 46, 6843−6851

■ ASSOCIATED CONTENT

Supporting Information

Additional chromatographic data and ^{1}H NMR spectra. This material is available free of charge via the Internet at http://pubs.acs.org.

■ AUTHOR INFORMATION

Corresponding Author

*E-mail steve.howdle@nottingham.ac.uk.

Notes

The authors declare no competing financial interest.

■ ACKNOWLEDGMENTS

The authors thank M. Hannah (University of Sheffield) for help and advice with the GPEC and M. C. Dellar, P. Fields, R. Wilson, and P. Gaetto for their technical and engineering input. We also thank the EPSRC for the PhD studentship (J.J.) and postdoctoral support (M.B.).

■ REFERENCES

(1) Ruiz, R.; Kang, H. M.; Detcheverry, F. A.; Dobisz, E.; Kercher, D. S.; Albrecht, T. R.; de Pablo, J. J.; Nealey, P. F. *Science* **2008**, *321* (5891), 936−939.

(2) Urbas, A.; Sharp, R.; Fink, Y.; Thomas, E. L.; Xenidou, M.; Fetters, L. J. *Adv. Mater.* **2000**, *12* (11), 812−814.

(3) Paquet, C.; Kumacheva, E. *Mater. Today* **2008**, *11* (4), 48−56.

(4) Kim, H. C.; Park, S. M.; Hinsberg, W. D. *Chem. Rev.* **2010**, *110* (1), 146−177.

(5) Jackson, E. A.; Hillmyer, M. A. *ACS Nano* **2010**, *4* (7), 3548−3553.

(6) Lu, A.; O'Reilly, R. K. *Curr. Opin. Biotechnol.* **2013**.

(7) Munoz-Bonilla, A.; Ali, S. I.; del Campo, A.; Fernandez-Garcia, M.; van Herk, A. M.; Heuts, J. P. A. *Macromolecules* **2011**, *44* (11), 4282−4290.

(8) Luo, Y. W.; Wang, X. G.; Zhu, Y.; Li, B. G.; Zhu, S. P. *Macromolecules* **2010**, *43* (18), 7472−7481.

(9) Braunecker, W. A.; Matyjaszewski, K. *Prog. Polym. Sci.* **2007**, *32* (1), 93−146.

(10) Destarac, M. *Macromol. React. Eng.* **2010**, *4* (3−4), 165−179.

(11) Oh, J. K. *J. Polym. Sci., Polym. Chem.* **2008**, *46* (21), 6983−7001.

(12) Cunningham, M. F. *Prog. Polym. Sci.* **2008**, *33* (4), 365−398.

(13) Jones, E. R.; Semsarilar, M.; Blanazs, A.; Armes, S. P. *Macromolecules* **2012**, *45* (12), 5091−5098.

(14) Zetterlund, P. B.; Aldabbagh, F.; Okubo, M. *J. Polym. Sci., Part A: Polym. Chem.* **2009**, *47* (15), 3711−3728.

(15) Wei, R.; Luo, Y.; Li, Z. *Polymer* **2010**, *51* (17), 3879−3886.

(16) Monteiro, M. J.; Sjoberg, M.; van der Vlist, J.; Gottgens, C. M. *J. Polym. Sci., Polym. Chem.* **2000**, *38* (23), 4206−4217.

(17) Chambon, P.; Blanazs, A.; Battaglia, G.; Armes, S. P. *Macromolecules* **2012**, *45* (12), 5081−5090. Altarawneh, I. S.; Gomes, V. G.; Srour, M. H. *Macromol. React. Eng.* **2012**, *6* (1), 8−16.

(18) Smulders, W.; Monteiro, M. J. *Macromolecules* **2004**, *37* (12), 4474−4483.

(19) Wei, R. Z.; Luo, Y. W.; Li, Z. S. *Polymer* **2010**, *51* (17), 3879−3886.

(20) Nicolas, J.; Ruzette, A. V.; Farcet, C.; Gerard, P.; Magnet, S.; Charleux, B. *Polymer* **2007**, *48* (24), 7029−7040.

(21) Farcet, C.; Charleux, B.; Pirri, R. *Macromolecules* **2001**, *34* (12), 3823−3826.

(22) Kagawa, Y.; Minami, H.; Okubo, M.; Zhou, H. *Polymer* **2005**, *46* (4), 1045−1049.

(23) Kitayama, Y.; Kagawa, Y.; Minami, H.; Okubo, M. *Langmuir* **2010**, *26* (10), 7029−7034.

(24) Kitayama, Y.; Kishida, K.; Minami, H.; Okubo, M. *J. Polym. Sci., Polym. Chem.* **2012**, *50* (10), 1991−1996.

(25) Kitayama, Y.; Yorizane, M.; Minami, H.; Okubo, M. *Polym. Chem.* **2012**, *3* (6), 1394−1398.

(26) Wang, W. W.; Zhang, Q. Y. *J. Colloid Interface Sci.* **2012**, *374*, 54−60. Luo, Y. D.; Chou, I. C.; Chiu, W. Y.; Lee, C. F. *J. Polym. Sci., Polym. Chem.* **2009**, *47* (17), 4435−4445. Tonnar, J.; Lacroix-Desmazes, P.; Boutevin, B. *Macromolecules* **2007**, *40* (17), 6076−6081.

(27) Robb, M. J.; Connal, L. A.; Lee, B. F.; Lynd, N. A.; Hawker, C. J. *Polym. Chem.* **2012**, *3* (6), 1618−1628.

(28) Yang, S.-M.; Kim, S.-H.; Lim, J.-M.; Yi, G.-R. *J. Mater. Chem.* **2008**, *18* (19), 2177−2190.

(29) Gregory, A. M.; Thurecht, K. J.; Howdle, S. M. *Macromolecules* **2008**, *41* (4), 1215−1222.

(30) Grignard, B.; Jerome, C.; Calberg, C.; Jerome, R.; Wang, W. X.; Howdle, S. M.; Detrembleur, C. *Macromolecules* **2008**, *41* (22), 8575−8583.

(31) Ryan, J.; Aldabbagh, F.; Zetterlund, P. B.; Okubo, M. *Polymer* **2005**, *46* (23), 9769−9777. McHale, R.; Aldabbagh, F.; Zetterlund, P. B.; Okubo, M. *Macromol. Chem. Phys.* **2007**, *208* (16), 1813−1822.

(32) Kuroda, T.; Tanaka, A.; Taniyama, T.; Minami, H.; Goto, A.; Fukuda, T.; Okubo, M. *Polymer* **2012**, *53* (6), 1212−1218.

(33) Jennings, J.; Beija, M.; Richez, A. P.; Cooper, S. D.; Mignot, P. E.; Thurecht, K. J.; Jack, K. S.; Howdle, S. M. *J. Am. Chem. Soc.* **2012**, *134* (10), 4772−4781.

(34) Minami, H.; Tanaka, A.; Kagawa, Y.; Okubo, M. *J. Polym. Sci., Polym. Chem.* **2012**, *50* (13), 2578−2584. O'Connor, P.; Yang, R. B.; Carroll, W. M.; Rochev, Y.; Aldabbagh, F. *Eur. Polym. J.* **2012**, *48* (7), 1279−1288.

(35) Barner-Kowollik, C. *Handbook of RAFT Polymerization*; Wiley-VCH: Weinheim, 2008. Matyjaszewski, K. *Macromolecules* **2012**, *45* (10), 4015−4039.

(36) Matyjaszewski, K.; Shipp, D. A.; McMurtry, G. P.; Gaynor, S. G.; Pakula, T. *J. Polym. Sci., Part A: Polym. Chem.* **2000**, *38* (11), 2023−2031.

(37) Bartels, J. W.; Cauet, S. I.; Billings, P. L.; Lin, L. Y.; Zhu, J. H.; Fidge, C.; Pochan, D. J.; Wooley, K. L. *Macromolecules* **2010**, *43* (17), 7128−7138.

(38) Gao, H. F.; Tsarevsky, N. V.; Matyjaszewski, K. *Macromolecules* **2005**, *38* (14), 5995−6004.

(39) Guo, R. W.; Shi, Z. P.; Wang, X. X.; Dong, A. J.; Zhang, J. H. *Polym. Chem.* **2012**, *3* (5), 1314−1321.

(40) Verhelst, V.; Vandereecken, P. *J. Chromatogr., A* **2000**, *871* (1−2), 269−277.

(41) Lai, J. T.; Filla, D.; Shea, R. *Macromolecules* **2002**, *35* (18), 6754−6756.

(42) Brandrup, J.; Immergut, E. H.; Grulke, E. A.; Abe, A.; Bloch, D. R. *Polymer Handbook*, 4th ed.; John Wiley & Sons: New York, 1999.

(43) Zhang, X. W.; Rieger, J.; Charleux, B. *Polym. Chem.* **2012**, *3* (6), 1502−1509.

(44) Shock, D.; Dennis, G. R.; Guiochon, G.; Dasgupta, P. K.; Shalliker, R. A. *Anal. Chim. Acta* **2011**, *703* (2), 245−249.

(45) Zetterlund, P. B.; Kagawa, Y.; Okubo, M. *Chem. Rev.* **2008**, *108* (9), 3747−3794.

(46) Monteiro, M. J.; Bussels, R.; Beuermann, S.; Buback, M. *Aust. J. Chem.* **2002**, *55* (6−7), 433−437. Arita, T.; Buback, M.; Janssen, O.; Vana, P. *Macromol. Rapid Commun.* **2004**, *25* (15), 1376−1381.

(47) Guan, Z. B.; Combes, J. R.; Menceloglu, Y. Z.; Desimone, J. M. *Macromolecules* **1993**, *26* (11), 2663−2669.

(48) Moad, G.; Rizzardo, E.; Thang, S. H. *Aust. J. Chem.* **2005**, *58* (6), 379−410.

(49) Zhong, M.; Matyjaszewski, K. *Macromolecules* **2011**, *44* (8), 2668−2677.

(50) Colby, R. H.; Fetters, L. J.; Graessley, W. W. *Macromolecules* **1987**, *20* (9), 2226−2237.

(51) Wissinger, R. G.; Paulaitis, M. E. *J. Polym. Sci., Part B: Polym. Phys.* **1987**, *25* (12), 2497−2510.

(52) Songkhla, P. N.; Wootthikanokkhan, J. *J. Polym. Sci., Part B: Polym. Phys.* **2002**, *40* (6), 562−571.

(53) Kitayama, Y.; Yorizane, M.; Kagawa, Y.; Minami, H.; Zetterlund, P. B.; Okubo, M. *Polymer* **2009**, *50* (14), 3182−3187.

(54) Li, M.; Min, K.; Matyjaszewski, K. *Macromolecules* **2004**, *37* (6), 2106−2112. Kagawa, Y.; Zetterlund, P. B.; Minami, H.; Okubo, M. *Macromolecules* **2007**, *40* (9), 3062−3069.